Development of a Visually Calculated SUV_{mean} (HIT Score) on Screening PSMA PET/CT to Predict Treatment Response to ^{177}Lu-PSMA Therapy: Comparison with Quantitative SUV_{mean} and Patient Outcomes

Mina Swiha[1,2], Nathan Papa[3], Zahra Sabahi[1], Narjess Ayati[1,3,4], Nikeith John[1,4], Sarennya Pathmanandavel[1], Megan Crumbaker[1,3–5], Sherrington Li[1], Shikha Agrawal[1], Maria Ayers[1], Adam Hickey[1], Shikha Sharma[1], Andrew Nguyen[1,4], and Louise Emmett[1,3,4]

[1]Department of Theranostics and Nuclear Medicine, St. Vincent's Hospital, Sydney, New South Wales, Australia; [2]Nuclear Medicine Division, Department of Medical Imaging, University of Western Ontario, London, Ontario, Canada; [3]Garvan Institute of Medical Research, Sydney, New South Wales, Australia; [4]St. Vincent's Clinical School, University of New South Wales, Sydney, New South Wales, Australia; and [5]Kinghorn Cancer Centre, St. Vincent's Hospital, Sydney, New South Wales, Australia

^{177}Lu-PSMA therapy is an effective treatment in patients with metastatic castration-resistant prostate cancer. SUV_{mean} is a valuable screening biomarker to assess the suitability for ^{177}Lu-PSMA therapy but requires quantitative software. This study aims to develop a simple, clinically applicable prostate-specific membrane antigen PET/CT score that encompasses the elements of SUV_{mean} without requiring additional quantification. **Methods:** Datasets from ethics-approved trials of patients with metastatic castration-resistant prostate cancer after androgen receptor signaling inhibition and taxane chemotherapy (or unfit for taxane), who were treated with ^{177}Lu-PSMA-617 and ^{177}Lu-PSMA I&T with a pretreatment screening with ^{68}Ga-PSMA-11 PET/CT, and clinical outcome data, including a prostate-specific antigen (PSA) 50% response rate (PSA50), PSA progression-free survival (PSA-PFS), and overall survival (OS), were included. The screening ^{68}Ga-PSMA-11 PET/CT of all participants was analyzed both semiquantitatively and visually. Semiquantitative analysis was used to derive the SUV_{mean}. Visual analysis of the ^{68}Ga-PSMA-11 PET/CT images involved a binary visual heterogeneity assessment (homogeneous or heterogeneous), allocating a tumor SUV_{max} range (<15, 15–29, 30–49, 50–79, or ≥80). A 4-category score incorporating both heterogeneity and intensity of tumors (HIT) was then developed as a combination of heterogeneity and intensity (SUV_{max} range). The SUV_{max} was less than 15 for score 1, 15–79 with heterogeneous intensity for score 2, 15–79 with homogeneous intensity for score 3, and 80 or greater for score 4. This score was evaluated according to clinical outcomes (PSA50, PSA-PFS, and OS) and compared with SUV_{mean}. **Results:** Data from 139 participants were analyzed. In total, 75 (54%) patients achieved a PSA50 with a median PSA-PFS of 5.5 mo (95% CI, 4.1–6.0 mo) and an OS of 13.5 mo (95% CI, 11.1–17.9 mo). SUV_{mean} was associated with PSA50 and survival outcomes when analyzed as a continuous variable or as quartiles. The PSA50 for HIT scores 1–4 was 0%, 39%, 65%, and 76%, respectively. The HIT score was strongly related to PSA-PFS and OS (log-rank test, $P < 0.001$ and $P = 0.002$). The median PSA-PFS for HIT scores 1–4 was 1.0, 4.1, 6.0, and 8.5, respectively, and the median OS was 7.6, 12.0, 18.5, and 16.9 mo, respectively. Cohen κ between readers for the HIT score was 0.71. **Conclusion:** A prostate-specific membrane antigen PET/CT score incorporating HIT derived from tools on a standard PET workstation is comparable with quantitative SUV_{mean} as a prognostic tool following ^{177}Lu-PSMA therapy.

Key Words: SUV_{mean}; prostate cancer; ^{177}Lu-PSMA; PSMA PET/CT

J Nucl Med 2024; 65:904–908
DOI: 10.2967/jnumed.123.267014

Treatment with ^{177}Lu-PSMA-617 improves the overall survival (OS) in men with metastatic castration-resistant prostate cancer (mCRPC) after androgen signaling inhibition and taxane chemotherapy (*1*). ^{177}Lu-PSMA is well tolerated and shows improved quality of life compared with second-line chemotherapy (*2*). Despite this, approximately one third of patients will have upfront treatment resistance or a limited duration of response to ^{177}Lu-PSMA radiopharmaceutical therapy (*3*). Developing imaging biomarkers to better predict response is important to further improve patient outcomes. The TheraP and VISION trials found that semiquantitatively derived SUV_{mean} from prostate-specific membrane antigen (PSMA) PET/CT imaging is predictive of treatment response with ^{177}Lu-PSMA-617 (*4–6*). However, deriving SUV_{mean} requires dedicated software programs not currently clinically available. The aim of this study is to develop a reproducible assessment method using standard PET workflow tools that correlates with SUV_{mean} and is predictive of patient outcomes with ^{177}Lu-PSMA.

MATERIALS AND METHODS

Study Population

This study is a retrospective analysis of screening ^{68}Ga-PSMA-11 PET/CT parameters and patient outcomes including prostate-specific membrane (PSA) 50% response rate (PSA50), PSA progression-free survival (PSA-PFS), and OS from 3 previously published clinical trials in men with progressive mCRPC who were undergoing ^{177}Lu-PSMA therapy after at least 1 line of androgen receptor signaling inhibition and 1 line of taxane chemotherapy or who were determined ineligible for taxane chemotherapy (*7–9*). The institutional review board of

Received Nov. 5, 2023; revision accepted Mar. 15, 2024.
For correspondence or reprints, contact Louise Emmett (louise.emmett@svha.org.au).
Published online Apr. 18, 2024.

St. Vincent's Hospital approved this retrospective study (Human Research Ethics Committee approval number 2022/ETH00924), and the requirement to obtain informed consent was waived.

PSMA PET/CT Acquisition and Visual Analysis

^{68}Ga-PSMA-11 PET/CT imaging was undertaken per institutional or clinical trial protocols before treatment with ^{177}Lu-PSMA. Images were analyzed both visually and semiquantitatively. Visual assessment included evaluation of heterogeneity and tumor intensity relative to parotid and liver avidity on rotating 3-dimensional maximum-intensity-projection images adjusted to the SUV window range (0–15). First, visual analysis was performed by 3 experienced nuclear medicine specialists who were masked to the clinical outcomes. Heterogeneity was a binary score. If at least 80% of all lesions not impacted by partial-volume effects (larger lesions) had similar intensities, this was classified as homogeneous. If more than 20% of larger lesions had variable intensity (inter- or intralesional), this was classified as heterogeneous (Fig. 1). Second, the readers measured the SUV_{max} of the most intense lesions and allocated an SUV_{max} range ($<$15, 15–29, 30–49, 50–79, or $\geq$80). Third, the readers evaluated if the most intense lesions were above the parotid intensity or between the liver and parotid intensities. No patients in whom the highest lesional intensity was below the liver intensity were enrolled. All readers participated in a 30-min training session that involved an explanation of the heterogeneity binary assessment and a consensus read of 20 ^{68}Ga-PSMA-11 PET/CT scans outside the study dataset. The heterogeneity category given by most readers was used for analysis.

PSMA PET/CT Quantitative Analysis

Semiautomated segmentation of baseline ^{68}Ga-PSMA-11 PET/CT was performed using MIM software (LesionID; MIM Software Inc.) and a standardized semiautomated workflow to delineate regions of interest with a minimum SUV_{max} cutoff of 3 and a lesion size of at least 0.5 mm. All lesions identified quantitatively were reviewed by experienced nuclear medicine physicians. Output parameters included SUV_{mean}, SUV_{max}, and total tumor volume.

Interreader Reliability

After development of the heterogeneity-and-intensity-of-tumors (HIT) score, a full reread of the same dataset was performed by an additional 2 experienced nuclear medicine specialists using HIT scores 1–4 with comparison of Cohen κ between these readers.

Clinical Outcomes

All patients were treated with ^{177}Lu-PSMA until they were no longer clinically benefiting. Clinical outcomes included PSA50, PSA-PFS, and OS. PSA50 was defined as a PSA decline of 50% or more compared with baseline at any time during the treatment. PSA-PFS was defined as the time from treatment initiation to PSA progression or death from any cause. PSA progression was defined as at least a 25% increase in PSA of at least 2.0 ng/mL above nadir per the criteria of the Prostate Cancer Clinical Trials Working Group 3 (*10*). OS was defined as the time from treatment initiation to death from any cause.

Statistical Analysis

The analysis followed 3 main phases. First, SUV_{mean} was confirmed as a predictor of outcomes in the sample by entering it continuously as a restricted cubic spline function with knots at the tertiles into a logistic (for PSA50) or Cox regression (for PSA-PFS and OS) and plotting the results. In the Cox regression, the (near) median value of 8 was set as the reference, and analysis time began on the date of cycle 1. Kaplan–Meier plots were also generated with SUV_{mean} entered as quartiles and log-rank tests used to identify differences in the survival curves. Second, the relation between SUV_{mean} and a combination of SUV_{max} range and visual heterogeneity was examined. Nested linear regression models and the likelihood ratio test were used to assess whether heterogeneity, above the SUV_{max} range alone, added significantly to the model fit predicting SUV_{mean}. A scatterplot with locally weighted regression curves of log-transformed SUV_{mean} versus SUV_{max} range, by heterogeneity, was generated to visually guide the creation of the 4-category HIT score. HIT score 1 was derived separately from the scatterplot on the basis of data demonstrating no PSA response in patients with an SUV_{max} less than 15 (*8*). HIT scores 2–4 were derived on the basis of the scatterplot. Score 4 required an SUV_{max} of at least 80 and was derived from the scatterplot as a point above which heterogeneous or homogeneous curves joined with no significant differences between the 2 groups—and with higher treatment responses. Finally, the relation between the 4-category HIT score and outcomes was assessed similarly to quartiles of SUV_{mean}. The predictive power of the Cox survival models including the HIT score, the quartiles of SUV_{mean}, or the quartiles of SUV_{max} range was quantified with the Somers D statistic. Exploratory analysis assessed the survival outcomes according to tumor intensity relative to parotid intensity with Kaplan–Meier plots and log-rank tests, and interrater agreement of the HIT score was calculated on the basis of image readings by 2 readers once the HIT score had been created. Analysis was performed with Stata/MP version 17.0 (StataCorp LLC), and tests were 2-sided with significance set at less than 0.05.

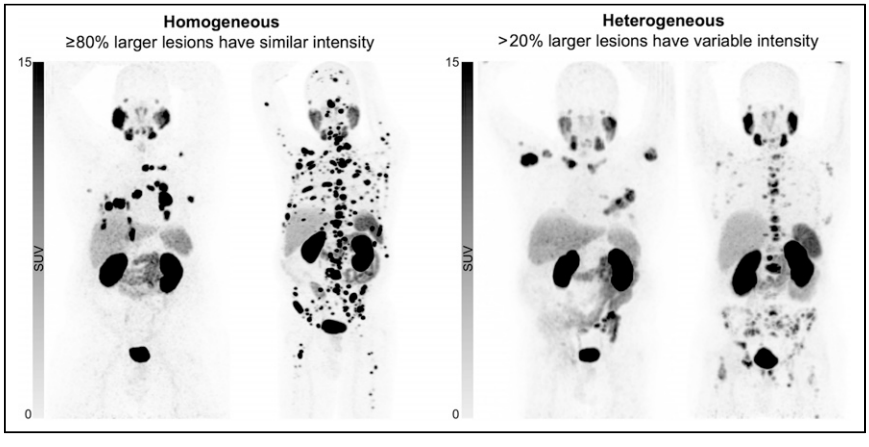

FIGURE 1. Maximum-intensity projection of PSMA PET/CT showing 2 patients with homogeneous PSMA uptake in lesions (left) and 2 patients with heterogeneous PSMA uptake in lesions (right).

RESULTS

Patient Characteristics

In total, 139 patients who had received ^{177}Lu-PSMA-617 or ^{177}Lu-PSMA I&T in two phase 2 clinical trials and a published clinical therapy program between 2016 and 2022 were included in this analysis (Table 1). All patients received a median of 4 doses of 7.5 GBq of ^{177}Lu-PSMA. The overall PSA50 was 54%, the number of PSA-PFS events was 120 with a median PSA-PFS of 5.5 mo (95% CI, 4.1–6.0 mo), and the number of deaths was 82, with a median OS of 13.5 mo (95% CI, 11.1–17.9 mo).

TABLE 1
Patient Characteristics

Characteristic	Value
n	139
Age (y)	69 (64–74)
Time since diagnosis (y)	6 (3–9)
ECOG status	
0–1	122 (88)
2	17 (12)
Baseline PSA (ng/mL)	94 (34–325)
LDH (NR, 120–250 U/L)	245 (216–317)
ALP (NR, 30–110 U/L)	112 (74–203)
Hemoglobin (NR, 130–180 g/L)	118 (106–129)
Previous systemic treatments	
Androgen receptor signaling inhibitors	139 (100)
Docetaxel	125 (90)
Cabazitaxel	88 (63)
Disease volume from PSMA PET/CT	
<20 metastases	49 (35)
≥20 metastases	90 (65)
Sites of disease on PSMA PET/CT	
Bone	133 (96)
Nodal*	72 (52)
Visceral	31 (22)

*Pelvic or distant.

ECOG = Eastern Cooperative Oncology Group; LDH = lactate dehydrogenase; NR = normal range; ALP = alkaline phosphatase.

Quantitative data are number and percentage. Continuous data are median and interquartile range.

SUV_{mean}

The median semiquantitatively derived SUV_{mean} was 8.0 (interquartile range, 6.6–9.9). Increasing SUV_{mean} as a continuous variable demonstrated a strong relationship with a higher probability of PSA50 and lower hazard ratio of PSA-PFS and OS, evidenced by a near-monotonic function with these outcomes (Supplemental Fig. 1; supplemental materials are available at http://jnm.snmjournals.org). When assessed as quartiles, SUV_{mean} significantly predicted PSA-PFS ($P < 0.001$) with borderline significance for OS ($P = 0.051$) (Fig. 2).

HIT Score

The 4-category HIT score was derived from an evaluation of heterogeneity and allocation of an SUV_{max} range. Inclusion of heterogeneity significantly improved the prediction of SUV_{mean} above that of the SUV_{max} range (likelihood ratio test, $P = 0.0041$); hence, both factors were required. On evaluation of the scatterplot and locally weighted regression curves (Fig. 3), in association with results from previous studies, the following categories were devised: score 1 was all patients with an SUV_{max} of less than 15; score 2 included patients defined as having heterogeneous disease visually with an SUV_{max} between 15 and 79; score 3 included patients with visually homogeneous disease and an SUV_{max} between 15 and 79; score 4 included all patients with an SUV_{max} of at least 80 independent of whether the tumor was homogeneous or heterogeneous (Fig. 4). The distribution of the HIT score among the sample was as follows: score 1, $n = 5$ (3.6%); score 2, $n = 54$ (39%); score 3, $n = 63$ (45%); and score 4, $n = 17$ (12%).

HIT-Score Agreement

Following HIT-score development, images were read by 2 readers and a score was assigned. The interrater agreement (Cohen κ) of the HIT score was 0.71 (95% CI, 0.60–0.82), and the percentage agreement was 82%.

HIT Score and Outcomes

The PSA50 for a HIT score of 1–4 was 0% (0/5), 39% (21/54), 65% (41/63), and 76% (13/17), respectively. The HIT score statistically significantly predicted both PFS and OS (log-rank test, $P < 0.001$ and $P = 0.002$, respectively) (Fig. 5). The differences in survival curves between scores 2 and 3 (same SUV_{max} range but heterogeneous vs. homogeneous) were also significant for PFS ($P < 0.001$) and OS ($P = 0.040$). The median PFS (95% CI) for HIT scores 1–4 was 1.0 mo (0.6 mo to not estimable), 4.1 mo (2.9–5.5 mo), 6.0 mo (5.1–9.4 mo), and 8.5 mo (3.3–14.5 mo), respectively. The corresponding median OS (95% CI) was 7.6 mo (5.5 mo to not estimable), 12.0 mo (8.9–17.9 mo), 18.5 mo (12.0–21.6 mo), and 16.9 mo (7.1 mo to not reached). Cox models with a HIT score had predictive power comparable to that of SUV_{mean} quartiles for PSA-PFS (Somers D of 0.25 vs. 0.27) and OS (Somers D of 0.15 vs. 0.16) and exceeded those for SUV_{max} range quartiles (0.17 for PFS and 0.12 for OS).

Physiologic Activity and Heterogeneity

Most patients had lesion intensity that was greater than parotid intensity, $n = 126$ (91%), with the remainder having an intensity between those of the liver and parotid. No statistically significant difference in survival curves for PSA-PFS or OS between those with intensity above or below that of the parotid was observed (Supplemental Fig. 2).

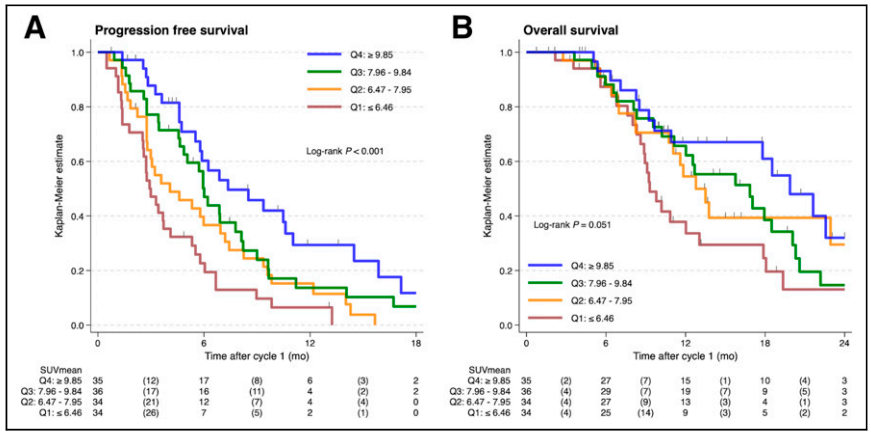

FIGURE 2. Kaplan–Meier curve (log-rank tests) of PSA-PFS (A) and OS (B) for semiquantitative SUV_{mean} quartiles (Q1–Q4).

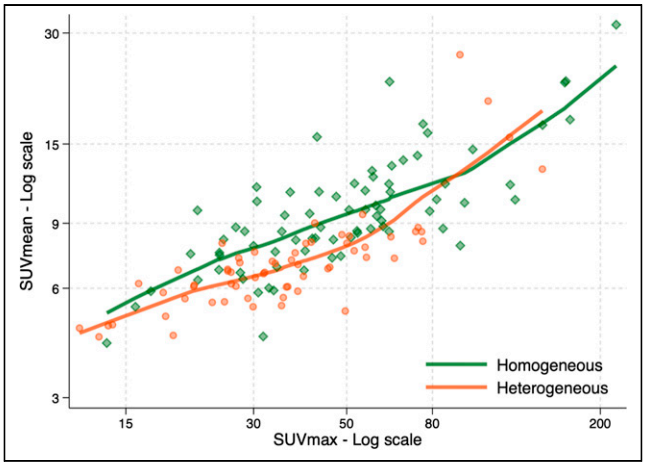

FIGURE 3. Scatterplot of weighted regression curves of log SUV_{mean} vs. SUV_{max} range, by visual heterogeneity score (homogeneous vs. heterogeneous).

	Intensity (SUV_{max})				
	<15	15-29	30-49	50-79	≥80
Heterogeneous	4	20	23	11	4
Homogeneous	1	14	24	25	13

FIGURE 4. Color-coded table of HIT scores 1–4 incorporating SUV_{max} range (most intense lesion) and binary visual heterogeneity with patient numbers in each group. Red = HIT score 1; yellow = HIT score 2; green = HIT score 3; blue = HIT score 4.

DISCUSSION

Developing screening imaging biomarkers that can predict response to ^{177}Lu-PSMA is important to improve patient outcomes and to better personalize treatment options. Quantitative whole-body SUV_{mean} has shown value in predicting treatment response in men treated with ^{177}Lu-PSMA in both TheraP and VISION trials; however, the clinical application of this tool is limited by the onerous requirements for image quantitation (*4*,*5*). This study has found that the HIT score, derived using tools available on clinical PET workstations, shows promising predictive capability for both PFS and OS in men being treated with ^{177}Lu-PSMA therapy.

SUV_{mean} is a semiquantitatively derived calculation of the mean voxel intensity of total-body tumor deposits. It gives a good measure of both the intensity of PSMA expression in tumor deposits and the variability of PSMA expression intra- and intertumorally. A patient with heterogeneous PSMA expression may have a low SUV_{mean} despite some deposits demonstrating high PSMA expression. Metastatic prostate cancer is inherently heterogeneous, with PSMA expression shown to be variable both within and between tumoral deposits (*11*). This heterogeneity could significantly impact the response to ^{177}Lu-PSMA (*12*). The HIT score using the most intense lesion SUV_{max} ranges with a binary visual tumor heterogeneity scoring on ^{68}Ga-PSMA PET/CT screening successfully predicts both PSA-PFS and OS in response to ^{177}Lu-PSMA therapy in men with mCRPC, with comparable predictability to quantitative SUV_{mean} quartiles.

Several previous studies have shown that PSMA SUV_{max} is not predictive of treatment response to ^{177}Lu-PSMA (*4*,*13*–*15*). However, these studies used PSMA SUV_{max} as a continuous or binary variable ($SUV_{max} < 20$ and ≥ 20). In this study, 5 ranges of PSMA SUV_{max} (<15, 15–29, 30–49, 50–79, and ≥80) were used. This was to allow better separation of intensity levels between patients and to reduce the impact of inherent limitations of SUV_{max} reproducibility. SUV_{max} is dependent on several variables that limit its reproducibility such as variation in body habitus, size of the maximal voxel between different scanners, and the statistical quality of the images (*16*). The HIT score, through combining a binary visual heterogeneity evaluation and SUV_{max} range, optimizes the clinical value of SUV_{max}, while minimizing the limitations of reproducibility.

The PSMA PET/CT tumor–to–salivary gland ratio proposed a visual method for assessment of tumor intensity using parotid intensity. A cohort of 237 patients was classified as high (>80% lesions above parotid), intermediate, and low (>80% lesions below parotid) (*13*). That study found that a high tumor-to–salivary gland ratio had higher PSA50 (63% vs. 17%) and longer PSA-PFS and OS than did the low tumor-to–salivary gland ratio (6.7 vs. 1.9 mo and 14.3 vs. 12.9 mo, respectively) (*13*). The current study shows no significant difference in patient outcome using PSMA intensity of the most active lesion above or below the parotid intensity but did not compare parotid with tumor intensity at all sites. Using whole-body lesions in tumor–to–salivary gland ratios provided an indirect measure of tumor heterogeneity and thus allowed stratification. HIT score integrating SUV_{max} ranges and binary heterogeneity score significantly correlates with PSA50 and both PSA-PFS and OS with higher separation between the highest and lowest scores in PSA50, PSA-PFS, and OS (76% vs. 0%, 8.5 vs. 1.0 mo, and 16.9 vs. 7.6 mo, respectively).

The current study has several limitations. Analysis of the screening ^{68}Ga-PSMA-11 PET/CT was undertaken retrospectively using data from single-institution trials. Results will need to be reproduced and validated in more diverse clinical datasets before clinical implementation, including full assessment of the reproducibility of the HIT score between multiple readers. Screening criteria for trial enrollment required minimal levels of PSMA intensity on ^{68}Ga-PSMA-11 PET/CT images; hence, the number of patients

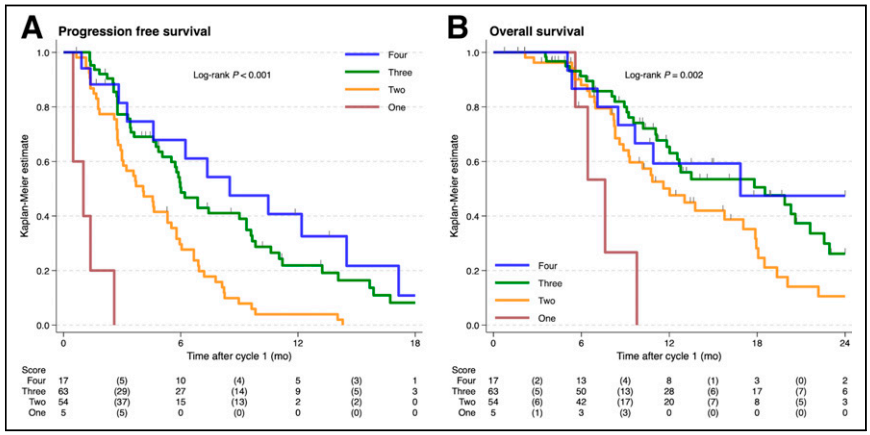

FIGURE 5. Kaplan–Meier curve (log-rank tests) of PSA-PFS (A) and OS (B) for HIT scores 1–4.

with an SUV_{max} less than 15 (HIT score 1) is low. ^{68}Ga-PSMA-11 was the only PET radiopharmaceutical used for screening patients in this study. The use of a heterogeneity score should be applicable across PSMA PET/CT ligands, and the use of the SUV_{max} range rather than using absolute SUV_{max} may mitigate differences between PSMA ligands, but this needs separate evaluation for confirmation.

CONCLUSION

A PSMA PET/CT score incorporating the HIT score derived from tools on a standard PET workstation is comparable to SUV_{mean} as a prognostic tool for PFS and OS following ^{177}Lu-PSMA therapy without the need for total-body quantitation. Further studies are warranted to validate the clinical utility of the HIT score.

DISCLOSURE

No potential conflict of interest relevant to this article was reported.

ACKNOWLEDGMENTS

We thank the patients and the clinical staff at the Department of Theranostics and Nuclear Medicine at St. Vincent's Hospital, Sydney, for their support.

KEY POINTS

QUESTION: Can a visually based score using standard PET workstation tools predict patient outcomes with ^{177}Lu-PSMA therapy on PSMA PET/CT screening and correlate with semiquantitative SUV_{mean}?

PERTINENT FINDINGS: The HIT score using standard PET workstation tools to measure tumor PSMA intensity and heterogeneity predicted PSA50, PSA-PFS, and OS and was comparable to quantitative SUV_{mean}.

IMPLICATIONS FOR PATIENT CARE: The HIT score is a simple clinically applicable PSMA PET/CT score that shows promising capability to predict patient outcomes with ^{177}Lu-PSMA therapy without requiring further quantification.

REFERENCES

1. Sartor O, de Bono J, Chi KN, et al. Lutetium-177-PSMA-617 for metastatic castration-resistant prostate cancer. *N Engl J Med.* 2021;385:1091–1103.
2. Hofman MS, Emmett L, Sandhu S, et al. [^{177}Lu]Lu-PSMA-617 versus cabazitaxel in patients with metastatic castration-resistant prostate cancer (TheraP): a randomised, open-label, phase 2 trial. *Lancet.* 2021;397:797–804.
3. Emmett L, John N, Pathmanandavel S, et al. Patient outcomes following a response biomarker-guided approach to treatment using ^{177}Lu-PSMA-I&T in men with metastatic castrate-resistant prostate cancer (Re-SPECT). *Ther Adv Med Oncol.* 2023; 15:17588359231156392.
4. Buteau JP, Martin AJ, Emmett L, et al. PSMA and FDG-PET as predictive and prognostic biomarkers in patients given [^{177}Lu]Lu-PSMA-617 versus cabazitaxel for metastatic castration-resistant prostate cancer (TheraP): a biomarker analysis from a randomised, open-label, phase 2 trial. *Lancet Oncol.* 2022;23:1389–1397.
5. Kuo PH, Hesterman J, Rahbar K, et al. [^{68}Ga]Ga-PSMA-11 PET baseline imaging as a prognostic tool for clinical outcomes to [^{177}Lu]Lu-PSMA-617 in patients with mCRPC: a VISION substudy. *J Clin Oncol.* 2022;40(suppl 16):5002.
6. Kuo PH, Morris M, Kendi AT, et al. Association of baseline quantitative [^{68}Ga]Ga-PSMA-11 PET imaging parameters with clinical outcomes in patients with mCRPC receiving [^{177}Lu]Lu-PSMA-617: a VISION sub-study [abstract]. *Eur J Nucl Med Mol Imaging.* 2023;50(suppl):S1–S898.
7. Crumbaker M, Pathmanandavel S, Yam AO, et al. Phase I/II trial of the combination of ^{177}lutetium prostate specific membrane antigen 617 and idronoxil (NOX66) in men with end-stage metastatic castration-resistant prostate cancer (LuPIN). *Eur Urol Oncol.* 2021;4:963–970.
8. Emmett L, Crumbaker M, Ho B, et al. Results of a prospective phase 2 pilot trial of ^{177}Lu-PSMA-617 therapy for metastatic castration-resistant prostate cancer including imaging predictors of treatment response and patterns of progression. *Clin Genitourin Cancer.* 2019;17:15–22.
9. John N, Pathmanandavel S, Crumbaker M, et al. ^{177}Lu-PSMA SPECT quantitation at 6 weeks (dose 2) predicts short progression-free survival for patients undergoing ^{177}Lu-PSMA-I&T therapy. *J Nucl Med.* 2023;64:410–415.
10. Scher HI, Morris MJ, Stadler WM, et al. Trial design and objectives for castration-resistant prostate cancer: updated recommendations from the Prostate Cancer Clinical Trials Working Group 3. *J Clin Oncol.* 2016;34:1402–1418.
11. Paschalis A, Sheehan B, Riisnaes R, et al. Prostate-specific membrane antigen heterogeneity and DNA repair defects in prostate cancer. *Eur Urol.* 2019;76:469–478.
12. Swiha M, Ayati N, Oprea-Lager DE, Ceci F, Emmett L. How to report PSMA PET. *Semin Nucl Med.* 2024;54:14–29.
13. Hotta M, Gafita A, Murthy V, et al. PSMA PET tumor-to-salivary gland ratio to predict response to [^{177}Lu]PSMA radioligand therapy: an international multicenter retrospective study. *J Nucl Med.* 2023;64:1024–1029.
14. Pathmanandavel S, Crumbaker M, Yam AO, et al. ^{177}Lu-PSMA-617 and idronoxil in men with end-stage metastatic castration-resistant prostate cancer (LuPIN): patient outcomes and predictors of treatment response in a phase I/II trial. *J Nucl Med.* 2022;63:560–566.
15. Seifert R, Seitzer K, Herrmann K, et al. Analysis of PSMA expression and outcome in patients with advanced prostate cancer receiving ^{177}Lu-PSMA-617 radioligand therapy. *Theranostics.* 2020;10:7812–7820.
16. Wahl RL, Jacene H, Kasamon Y, Lodge MA. From RECIST to PERCIST: evolving considerations for PET response criteria in solid tumors. *J Nucl Med.* 2009;50 (suppl 1):122S–150S.